Multifaceted mechanisms regulating *Brassica oleracea* growth under shading gradients in an agrivoltaic system: Integrated responses of the soil-plant system and transcriptomic analysis

Zhuo Chen, Xiaocui Liu, Tiantian Ban, Chao Ma*

(*Guizhou Academy of Agricultural Sciences Horticultural Research Institute (Guizhou Province Horticulture Engineering Technology Research Center), Guiyang 550025, China*)

Abstract: Agrivoltaic systems represent a sustainable land-use paradigm capable of synergistically generating electricity and producing agricultural crops on the same piece of land. However, the mechanisms by which photovoltaic shading affects crop growth are not fully understood. This study investigated these mechanisms using *Brassica oleracea* as a model plant at an agrivoltaic base in Guizhou Province, China. Treatments included high shading (HP, 70%-80%), low shading (LP, 20%-30%), and no shading (NP). This study systematically examined the regulatory effects of these shading gradients on soil physicochemical properties, plant growth physiology, and transcriptomic expression. Results indicated that the NP treatment yielded the highest *B. oleracea* biomass, while the LP treatment significantly enhanced the content of quality components such as sugars and starch while maintaining a relatively high yield. The HP treatment promoted the accumulation of structural substances (cellulose, lignin) and maintained higher soil nutrient levels. Transcriptome analysis revealed that shading significantly altered pathways involved in photosynthesis, starch and sucrose metabolism, and plant hormone signal transduction. Several key responsive genes were identified, including Bo4g182560 (a chlorophyll a/b-binding protein) and Bo3g039200 (involved in jasmonic acid biosynthesis). Furthermore, different shading environments induced distinct antioxidant strategies: the NP zone relied on peroxidase (POD) activity to manage oxidative pressure associated with full sunlight exposure, whereas the HP zone maintained redox homeostasis by enhancing catalase (CAT) activity. By integrating multi-omics data spanning soil, plant, and molecular levels, this study partially elucidates the adaptive regulatory network of *B. oleracea* in the agrivoltaic system, specifically involving photosynthesis, starch and sucrose metabolism, plant hormone signal transduction, and distinct antioxidant strategies, providing a theoretical basis and genetic resources for system optimization and precise crop configuration.

Keywords: agrivoltaic system, shading gradient, *Brassica oleracea*, soil physicochemical properties, crop physiology, transcriptomics

DOI: 10.25165/j.ijabe.20261904.10486

Citation: Chen Z, Liu X C, Ban T T, Ma C. Multifaceted mechanisms regulating *Brassica oleracea* growth under shading gradients in an agrivoltaic system: Integrated responses of the soil-plant system and transcriptomic analysis. Int J Agric & Biol Eng, 2026; 19(4): 152–164.

1 Introduction

Food security is a cornerstone of human survival and global development, as well as a central prerequisite for poverty eradication and sustainable development. However, hunger remains a critical issue worldwide, with some regions experiencing persistent shortfalls in food supply. Against this backdrop, ensuring stable and reliable food provision has become increasingly urgent[1]. At the same time, the energy sector is confronting serious challenges. Accelerating urbanization and continued population growth have exacerbated carbon emissions, making the transition to renewable energy an essential pathway toward achieving carbon neutrality[2]. While the large-scale deployment of clean energy technologies such as wind and solar power is crucial for a green energy transition, these installations require substantial land resources. Concurrently, agricultural expansion and protection also depend on finite land availability[3]. Consequently, against a backdrop of growing land constraints, competition between energy transition and food security for land resources is becoming increasingly apparent. Coordinating these competing demands and achieving synergistic optimization of the "energy–food–land" nexus has emerged as a vital issue for sustainable development. Agrivoltaic systems, which integrate electricity generation and agricultural production on the same land area, present a promising solution to this dilemma, enabling effective energy transition without compromising agricultural development[4].

The conceptual foundation of agrivoltaic systems dates back to the pioneering work of German researchers Goetzberger and Zastrow in 1981. They pioneered the systematic demonstration of the feasibility of combining photovoltaic (PV) infrastructure with agricultural production from the perspective of light-use efficiency, laying a critical theoretical foundation for subsequent technological development[5]. At that time, however, significant conflict between

Received date: 2026-02-02 **Accepted date:** 2026-08-06

Biographies: **Zhuo Chen**, Assistant Research Fellow, research interest: vegetable cultivation and physiology, Email: 727560874@qq.com; **Xiaocui Liu**, Assistant Research Fellow, research interest: vegetable cultivation and physiology, Email: 651078369@qq.com; **Tiantian Ban**, Assistant Research Fellow, research interest: Vegetable cultivation and physiology, Email: 1574601087@qq.com.

***Corresponding author: Chao Ma**, Research Fellow, research interest: vegetable cultivation and physiology. Horticultural Research Institute, Guizhou Academy of Agricultural Sciences, Guiyang 550025, China. Tel: +86-13511979130, Email: machao621@126.com.

agricultural and energy land uses had not yet emerged, and there was insufficient urgency to drive widespread adoption of such systems. As a result, progress remained slow.

Since the beginning of the 21st century, the global energy transition has accelerated. With the scale-up of solar power as a prominent renewable energy source, competition for land has become more pronounced. In this context, agrivoltaic systems—which co-locate PV infrastructure and crop production—not only help alleviate land use pressure but also leverage panel shading to modulate microclimates and optimize crop growth environments[6]. Furthermore, such systems align with the United Nations Sustainable Development Goals, particularly "Zero Hunger" and "Affordable and Clean Energy," thereby garnering increasing attention from both the academic community and policymakers worldwide. The application scale of agrivoltaics continues to expand globally[7].

A central research focus in agrivoltaics is the shading effect induced by PV panels and its impact on crop growth. Light is a key environmental factor determining crop yield and quality[8]. PV shading not only directly influences photosynthesis and final crop output but also indirectly affects growth and quality by altering canopy microenvironments and soil conditions. International studies illustrate the complex and crop-specific nature of shading effects: i.g., an agrivoltaic trial in northern Colorado, USA, showed that zucchini yield decreased significantly under shading, while peppers, tomatoes, and lettuce exhibited no significant reduction, with most crops producing higher yields under increased light exposure[9]; in a Nigerian system, PV shading reduced photosynthetically active radiation and leaf temperature in mung beans, while increasing relative humidity and enhancing their maximum photochemical efficiency[10]; an Italian study on dynamic agrivoltaic systems found that shaded areas exhibited reduced crop evapotranspiration, and although continuous shading decreased fresh biomass in some plants, essential oil production was higher, indicating that for certain crops, agrivoltaics can not only sustain but even enhance high-value product output[11]; research in China demonstrated that by homogenizing light distribution and supplementing with LED lighting, agrivoltaic systems can maintain lettuce growth and yield while improving quality[12]. Thus, the effects of PV shading vary considerably depending on crop type, shading intensity, and environmental management strategies: excessive shading may reduce yield, yet moderate shading may improve crop quality. A study in the United States also showed that PV shading significantly affects soil physicochemical properties and microbial community structure and function in grasslands[13]. These findings highlight that PV installations influence not only crops but also soil properties, suggesting that soil-mediated indirect effects may further modulate crop performance under agrivoltaic conditions.

Meanwhile, transcriptomics-based research has gradually been applied in agrivoltaic systems to elucidate molecular mechanisms underlying crop responses to shading stress. In a study on *Leymus chinensis*, physiological and transcriptomic analyses compared the responses of two genotypes under shading, revealing that starch and sucrose metabolism and glycolysis/gluconeogenesis were common core enriched pathways, while flavonoid biosynthesis and galactose metabolism were more prominently enriched in the shade-tolerant genotype. The study identified LcGolS2, encoding galactinol synthase, as a potential hub gene conferring shade tolerance[14]. Research on leaf-used sweet potato investigated effects under varying shading levels; transcriptome analysis indicated that expression of genes related to antioxidant activity, phenolic and flavonoid secondary metabolism, photosynthesis, and MAPK signaling pathways varied with shading intensity. For instance, 30% shading induced high expression of antioxidant genes, 50% shading up-regulated genes involved in phenolic and flavonoid metabolism, and under 70% shading, MAPK signaling was regulated with down-regulation of most stress-related genes, while photosynthesis-related genes were up-regulated with increasing shade[15]. These studies provide molecular-level insights into the adaptive mechanisms of different crops under agrivoltaic shading environments.

However, current research tends to focus on isolated dimensions: some studies concentrate on the regulation of crop yield and quality by PV shading; others are limited to its effects on soil physicochemical properties and microbial community structure and function; while yet others only screen genes via physiological and transcriptomic approaches. There is a notable lack of integrated and systematic analysis. To address this gap, this study uses *Brassica oleracea* as a model system and employs a multi-dimensional experimental design to systematically decipher the mechanisms of shading effects. At the soil level, four treatments were established: high shade (HP), low shade (LP), no shade (NP), and a high shade no-crop control (CK). Eleven soil physicochemical indicators were measured before planting and after harvest to clarify the pure shading effect on the soil environment and the crop-soil interaction. At the plant phenotype and physiology level, three treatments (HP, LP, NP) were used to comprehensively assess agronomic traits, yield, 11 physiological quality indicators, and five antioxidant indicators, providing a holistic evaluation of shading impact on *B. oleracea* growth. For molecular mechanisms, under the same three shading treatments, transcriptomics (RNA-seq) was applied to identify differentially expressed genes in leaves and to screen candidate genes associated with key pathways such as photosynthesis, stress response, and hormone signaling. Furthermore, 10 key genes were validated via qRT-PCR to ensure the reliability of omics findings and to solidify evidence for the molecular regulatory mechanisms underlying shade stress responses. By integrating multi-dimensional data from soil, physiology, and transcriptomics, this study constructs a complete response chain from "environmental driver" to "physiological response" and further to "molecular regulation," aiming to provide a theoretical basis and data support for optimizing crop configuration in agrivoltaic systems and enhancing their overall benefits.

2 Materials and methods

2.1 Experimental site and design

2.1.1 Site description and duration

The field experiment was conducted at the Xianshuiwo Agrivoltaic Demonstration Base in Shuanglong Town (26.80°N, 104.08°E), Weining Yi, Hui, and Miao Autonomous County, Guizhou Province, China, situated at an altitude of over 2200 meters above sea level. The experiment spanned from February 2025 to July 2025.

2.1.2 Climate

The experimental site experiences a subtropical monsoon humid climate. However, due to the high altitude, it is characterized by cool summers, ample sunshine, abundant precipitation, and concurrent rainfall and heat periods. The mean annual temperature ranges from 10°C to 14°C, with annual precipitation of approximately 900-1000 mm and annual sunshine duration of about 1500-2000 h.

2.1.3 Photovoltaic (PV) facility description

The PV power station was constructed by the end of 2019 and

has been operational since then. Prior to PV installation, the area was managed as conventional farmland for many years under consistent tillage, fertilization, and irrigation regimes, resulting in relatively uniform soil properties across the site. Monocrystalline silicon modules (Model: JKM315M-60-V; 315 W; 1650×992×35 mm) manufactured by Jinko Solar Holding Co., Ltd. were used. The spacing between adjacent PV panel arrays was 8.4 m.

2.1.4 Experimental design

The experimental field followed an annual crop rotation of Chinese cabbage - *B. oleracea* - buckwheat. The preceding Chinese cabbage crop was planted in October 2024 and harvested in early February 2025, after which the land lay fallow. In mid-February 2025, the field underwent comprehensive soil preparation, including deep plowing to a depth of 30 cm and mechanical removal of all residual crop roots and weeds to ensure loose soil free from competitive vegetation.

A randomized complete block design with three replications was employed. Four treatments were established:

HP (High shading plot): *B. oleracea* was cultivated directly beneath the PV panels.

LP (Low shading plot): *B. oleracea* was planted in the middle of the space between two PV panel arrays.

NP (No shading plot): *B. oleracea* was grown in full sunlight without any PV panel shading.

CK (Control): No crops were planted in the high shading area (~70%–80% shading rate). This treatment was included solely for analyzing soil physicochemical properties.

Shading rates were estimated based on the geometric configuration of the PV array. The panels (1.650 m×0.992 m) were mounted at a 20° tilt angle, with the lower edge 1.4-1.8 m (mean 1.6 m) above ground and an inter-row spacing of 8.4 m. Field measurements indicated that the vertical projection of the PV panels spanned 3.2 m per array row, covering 39.0% of the total land area. Based on this configuration and the spatial positions of the plots, the HP zone (directly beneath the panels) was estimated to receive predominantly diffuse radiation, corresponding to a shading rate of approximately 70%-80%; the LP zone (midpoint between two adjacent arrays) received direct radiation during most of the day with partial shading in the early morning and late afternoon, corresponding to approximately 20%-30% shading; and the NP zone (well outside the panel coverage area) served as the 0% shading reference. This geometric estimation approach is consistent with methods described for shading characterization in solar energy systems[16]. It is noted that these estimates reflect the geometric light interception potential and may not fully capture diurnal and seasonal dynamics of actual photosynthetically active radiation, which is a limitation.

The test *B. oleracea* cultivar 'Xiaotietou' was transplanted into the HP, LP, and NP plots in early March 2025. The cultivation employed plastic film mulching, with a row spacing of approximately 20 cm and plant spacing of approximately 15 cm. Before transplanting, all plots (including CK) uniformly received 1000 kg/hm^2 of dried cattle manure as a base fertilizer. Subsequently, all HP, LP, NP, and CK plots received topdressing with equal amounts of 15-15-15 (N-P-K) compound fertilizer in early April and mid-May. Throughout the growing season, agricultural practices such as irrigation and pest control were maintained consistently across all planting treatments (HP, LP, NP).

Soil samples were collected at two time points: (1) before planting (February 2025, designated HP1, LP1, NP1, CK1) and (2) after harvest (July 2025, designated HP2, LP2, NP2, CK2). All soil samples were collected from the 0-20 cm topsoil layer. Measurements of agronomic traits, yield, quality, antioxidant indicators, and subsequent transcriptomic analysis were conducted only for the HP, LP, and NP treatments.

2.2 Soil sampling and analysis

Soil samples from the 0-20 cm depth were collected from each plot before *B. oleracea* planting (February 2025) and after harvest (July 2025). A portion of the fresh soil was immediately used to determine physical properties such as soil water content and bulk density. The remaining samples were air-dried, ground, and sieved for analysis of routine chemical properties. Specifically, soil total nitrogen was determined using the Kjeldahl method after sulfuric acid digestion[17]. Soil alkaline hydrolyzable nitrogen was measured by the alkali hydrolysis diffusion method[18]. Soil available phosphorus in acidic soil was determined using the NH_4F-HCl method[19]. Soil total phosphorus was measured by NaOH alkali fusion followed by the molybdenum-antimony anti-spectrophotometric method[20]. Soil total potassium was determined by NaOH alkali fusion and flame photometry[21]. Soil available potassium was extracted with ammonium acetate solution and measured by flame photometry[22]. Soil electrical conductivity (EC) was determined using the electrode method[23]. Soil pH was measured potentiometrically[24]. Soil organic matter content was determined by the potassium dichromate oxidation-external heating method[25]. Soil bulk density, maximum water holding capacity, and porosity were measured using the core method[26]. Soil water content was determined gravimetrically[27].

2.3 Measurement of plant agronomic traits and physiological indicators

At harvest, representative and uniformly growing plants from each replicate plot per treatment were selected for destructive sampling and measurement. Six plants per treatment were used for agronomic trait and yield determination, while three plants per treatment were used for quality and antioxidant indicator analysis.

Plant height, head transverse diameter, head vertical diameter, leaf length, and leaf width were measured using a measuring tape. The number of leaves was counted directly. Single head weight was measured using an electronic balance, and yield per unit area was calculated. The relative chlorophyll content of functional leaves was determined using a SPAD chlorophyll meter. Samples for physiological and biochemical analysis were taken from the head leaves, rapidly frozen in liquid nitrogen, and stored at –80°C until analysis. Soluble sugar content was determined by the anthrone colorimetric method[28]. Reducing sugar content was measured using the 3,5-dinitrosalicylic acid (DNS) colorimetric method[29]. Total sugar and starch contents were determined by acid hydrolysis followed by the anthrone colorimetric method[30]. Sucrose content was measured by the resorcinol colorimetric method[31]. Polysaccharide content was determined by the phenol-sulfuric acid method[32]. Glucose content was assayed using the glucose oxidase-peroxidase method[33]. Fructose content was measured by high-performance liquid chromatography (HPLC)[34]. Cellulose content was determined by the anthrone colorimetric method[35]. Hemicellulose content was measured by the sulfuric acid-anthrone colorimetric method[36]. Lignin content was determined using the acetyl bromide method[37]. Regarding the antioxidant system: Superoxide dismutase (SOD) activity was assayed by the nitroblue tetrazolium (NBT) photoreduction method[38]. Catalase (CAT) activity was measured by ultraviolet spectrophotometry[39]. Peroxidase (POD) activity was determined using the guaiacol method[40]. Malondialdehyde (MDA) content was measured by the

thiobarbituric acid (TBA) colorimetric method[41]. Hydrogen peroxide (H_2O_2) content was determined by the titanium sulfate colorimetric method[42].

2.4 Transcriptome sequencing and analysis

At harvest, fresh young leaf tissues were collected from three uniformly growing, representative plants from each of the HP, LP, and NP treatments. The samples were immediately frozen in liquid nitrogen and stored at –80°C for transcriptome sequencing analysis.

Total RNA was extracted from plant samples using a combined CTAB and pBIOZOL Plant Total RNA Extraction Reagent method. RNA was accurately quantified using a Qubit 4.0 Fluorometer, and RNA integrity was assessed using a Qsep400 High-Throughput Nucleic Acid Analysis System to ensure all samples met the library construction standards. Subsequently, mRNA with polyA tails was enriched using VAHTS mRNA Capture Beads 2.0 via Oligo(dT) beads. The enriched mRNA was fragmented, and first-strand cDNA was synthesized using random hexamer primers. During second-strand synthesis, dUTP was incorporated instead of dTTP for strand-specific library construction. The resulting cDNA underwent end repair, A-tailing, and sequencing adapter ligation. Fragments of 250–350 bp were selected using VAHTS DNA Clean Beads. Final library preparation was completed on an MGISP-960 automated workstation, and sequencing was performed on the DNBSEQ-T7 platform, generating 150 bp paired-end reads.

Raw sequencing data were quality-controlled using fastp to obtain high-quality clean reads. The clean reads were then aligned to the *B. oleracea* reference genome[43] using HISAT2 software. Transcript assembly and gene expression level quantification were performed using StringTie and featureCounts[44]. Differential expression analysis between groups was conducted using DESeq2 software, with a significance threshold set at an adjusted *p*-value (FDR)<0.05 and $|\log_2\text{FoldChange}|\geq 1$[45]. The identified differentially expressed genes (DEGs) were subjected to Gene Ontology (GO) functional enrichment and Kyoto Encyclopedia of Genes and Genomes (KEGG) pathway enrichment analyses[46,47].

Additionally, differential alternative splicing events between groups, including skipped exon, retained intron, mutually exclusive exon, alternative 5’ splice site, and alternative 3’ splice site, were analyzed using rMATS[48]. SNP detection was performed using GATK, and the variant sites were annotated with ANNOVAR. A protein-protein interaction (PPI) network for the DEGs was constructed based on the STRING database. Gene Set Enrichment Analysis (GSEA) and Weighted Gene Co-expression Network Analysis (WGCNA) were also employed to systematically investigate gene regulatory relationships and functional modules.

2.5 qRT-PCR validation

To independently verify the reliability of the transcriptome sequencing results, 10 key DEGs were selected for qRT-PCR analysis[49]. The *B. oleracea* samples used were the same as those used for transcriptome sequencing. The methods for total RNA extraction and detection were consistent with those described in section 2.4. Genomic DNA removal and first-strand cDNA synthesis were performed using a Bioground Reverse Transcription Kit (BG0070). The reaction mixture consisted of 1 μg total RNA, 4 μL 5×Reaction Mix, 3 μL Supreme Enzyme Mix, and DEPC water to a final volume of 20 μL. The reverse transcription program was set as follows: 25°C for 10 min, 55°C for 15 min, and 85°C for 5 min. The resulting cDNA products were diluted 20-fold with sterile water and used as templates for qPCR. Quantitative real-time PCR was performed using Bioground SYBR Green Premix (BG0014) on a Bio-Rad CFX96 Real-Time PCR System. The reaction mixture contained 10 μL of 2× SP qPCR Mix, 0.5 μL of forward primer (10 μM), 0.5 μL of reverse primer (10 μM), and ddH_2O to a final volume of 20 μL. The amplification protocol was as follows: initial denaturation at 94°C for 20 s, followed by 40 cycles of denaturation at 94°C for 10 s, and annealing/extension at 60°C for 20 s. The *B. oleracea* Actin gene was used as the internal reference[50]. The relative expression levels of the target genes were calculated using the $2^{(-\Delta\Delta Ct)}$ method[51]. Each sample was run with three technical replicates, and the experiment was independently repeated three times.

3 Results

3.1 Dynamic effects of different shading and planting treatments on soil physicochemical properties

3.1.1 Differences in soil physicochemical properties among different zones before *B. oleracea* planting

The soil quality parameters measured before the planting of *B. oleracea* are presented in Table 1. NP1 exhibited significantly lower alkaline-hydrolyzable nitrogen and total nitrogen than the other treatment groups ($p<0.05$), whereas available phosphorus and available potassium were highest in NP1 and lowest in HP1 (Table 1).

Table 1 Soil quality parameters across different treatment groups before *B. oleracea* planting

Parameter	HP1	LP1	NP1	CK1
PH	5.78±0.03^{a}	5.49±0.12^{a}	5.97±0.70^{a}	5.94±0.09^{a}
Alkaline-hydrolyzable N/mg·kg^{-1}	302.33±8.80^{a}	299.96±3.84^{a}	249.69±14.05^{b}	296.91±9.43^{a}
Available P/mg·kg^{-1}	30.63±6.07^{c}	42.15±3.31^{b}	51.25±2.25^{a}	14.64±3.23^{d}
Available K/mg·kg^{-1}	67.91±2.02^{c}	163.06±10.48^{b}	233.00±14.54^{a}	162.24±5.02^{b}
Total N/mg·g^{-1}	4.82±0.13^{a}	4.86±0.09^{a}	3.94±0.14^{b}	4.82±0.12^{a}
Total P/g·kg^{-1}	0.98±0.07^{a}	0.97±0.01^{a}	0.98±0.04^{a}	1.00±0.13^{a}
Total K/g·kg^{-1}	9.39±0.41^{a}	9.26±0.59^{a}	9.06±0.39^{a}	9.55±1.01^{a}
EC/μS·cm^{-1}	63.00±12.53^{b}	163.03±94.75^{ab}	315.73±135.21^{a}	74.87±16.44^{b}
Soil organic matter/g·kg^{-1}	99.21±1.70^{b}	99.06±0.96^{b}	72.93±4.92^{c}	107.62±3.31^{a}
Soil organic carbon/g·kg^{-1}	57.55±0.99^{b}	57.46±0.56^{b}	42.30±2.86^{c}	62.43±1.92^{a}
Water content/%	26.83±1.16^{b}	27.15±0.49^{b}	17.47±2.97^{c}	32.23±0.67^{a}
Maximum water holding capacity/g·kg^{-1}	840.50±81.57^{ab}	820.37±22.29^{b}	595.07±49.70^{c}	920.87±22.50^{a}
Bulk density/g·cm^{-3}	0.82±0.40^{b}	0.81±0.17^{b}	0.96±0.46^{a}	0.74±0.20^{c}
Porosity/%	68.13±3.53^{a}	66.50±0.40^{a}	57.17±2.15^{b}	68.30±0.69^{a}

For soil physical properties, CK1 and NP1 represented two contrasting extremes: CK1 had the highest organic matter, water content, and water holding capacity with the lowest bulk density, whereas NP1 showed the opposite pattern; HP1 and LP1 fell between these extremes (Table 1).

These results indicate that, even before planting, the different shading zones and the presence or absence of planting significantly affected both soil nutrient content and physical properties. The no-shading zone exhibited higher available nutrient content but poorer physical structure, whereas the high-shading zone demonstrated superior water retention capacity and a looser soil structure.

3.1.2 Differences in soil physicochemical properties among different zones at *B. oleracea* harvest

Soil quality parameters measured at the harvest of *B. oleracea* are presented in Table 2. At harvest, HP2 maintained the highest alkaline-hydrolyzable nitrogen, available phosphorus, total nitrogen,

and organic matter among all treatments, whereas NP2 showed the lowest values for these indicators. CK2 retained superior water holding capacity. No significant differences were observed in available potassium, bulk density, or porosity among treatments (Table 2).

Table 2 Soil quality parameters across different treatment groups at *B. oleracea* harvest

Parameter	HP2	LP2	NP2	CK2
PH	5.01±0.14^{b}	4.9767±0.51^{b}	6.84±0.75^{a}	5.42±0.23^{b}
Alkaline-hydrolyzable N/mg·kg^{-1}	301.11±31.53^{a}	264.18±17^{ab}	185.22±52.77^{c}	213.36±13.50^{cb}
Available P/mg·kg^{-1}	56.14±10.02^{a}	25.48±5.66^{c}	39.32±4.62^{b}	31.05±3.15^{cb}
Available K/mg·kg^{-1}	163.33±58.97^{a}	153.67±34.03^{a}	133.67±37.07^{a}	217.67±96.99^{a}
Total N/mg·g^{-1}	4.13±0.06^{a}	3.83±0.09^{a}	2.8±0.54^{b}	3.29±0.12^{b}
Total P/g·kg^{-1}	2.91±0.17^{a}	2.66±0.31^{a}	1.54±0.64^{b}	2.24±0.12^{ab}
Total K/g·kg^{-1}	16.23±6.09^{a}	15.13±3.30^{a}	13.13±3.60^{a}	21.57±9.75^{a}
EC/μS·cm^{-1}	316.53±257.33^{a}	283.33±142.86^{a}	237.87±200.23^{a}	95.23±13.22^{a}
Soil organic matter/g·kg^{-1}	91.77±5.82^{a}	73.8±2.43^{ab}	39.03±17.67^{c}	66.53±9.65^{b}
Soil organic carbon/g·kg^{-1}	53.27±3.41^{a}	42.83±1.45^{ab}	22.63±10.25^{c}	38.57±5.56^{b}
Water content/%	27.96±0.90^{ab}	30.27±1.16^{a}	23.06±6.00^{b}	28.54±0.52^{ab}
Maximum water holding capacity/g·kg^{-1}	763.33±12.79^{ab}	712.63±21.53^{c}	742.3±10.62^{b}	781.73±15.40^{a}
Bulk density/g·cm^{-3}	0.77±0.06^{a}	0.82±0.05^{a}	0.83±0.04^{a}	0.78±0.01^{a}
Porosity/%	58.83±4.74^{a}	58.7±3.65^{a}	61.67±2.40^{a}	60.77±1.72^{a}

In terms of soil organic matter and physical properties, the organic matter content in HP2 (91.77 g/kg) was significantly higher than that in NP2 (39.03 g/kg) and CK2 (66.53 g/kg). The maximum water holding capacity in CK2 (781.73 g/kg) was significantly higher than that in LP2 and NP2, indicating a relatively better water retention capacity. No significant differences were detected in bulk density or porosity among the treatments.

These results demonstrate that after one season of *B. oleracea* cultivation, the high-shading planting zone (HP) exhibited a clear advantage in maintaining soil nutrient levels, particularly in available phosphorus and alkaline-hydrolyzable nitrogen content, which were significantly higher than in other treatments. Meanwhile, the high-shading no-plant treatment (CK) retained a certain advantage in terms of physical water retention capacity.

3.1.3 Dynamic impact of *B. oleracea* cultivation in the agrivoltaic system on soil quality

The results of the temporal dynamic analysis of soil quality are presented in Table 3. Across the growing season, ΔHP consistently showed the smallest decreases in alkaline-hydrolyzable nitrogen, total nitrogen, organic matter, and organic carbon, and was the only treatment to show increases in available phosphorus and available potassium, indicating superior nutrient retention. In contrast, ΔNP showed the greatest nutrient depletion but was the only treatment to exhibit improved soil physical properties, including significant increases in maximum water holding capacity (+147.23 g/kg), porosity (+4.52%), and a decrease in bulk density (–0.13 g/cm^{3}). ΔCK experienced the largest nutrient losses overall (Table 3).

These results indicate that after one season of *B. oleracea* cultivation, the different treatments had distinct impacts on soil quality evolution: the high-shading planting (HP) treatment performed best in maintaining nutrient contents (such as nitrogen, phosphorus, and potassium) and exhibited the smallest consumption of organic matter. In contrast, the no-plant (CK) treatment experienced greater nutrient loss. Although the no-shading planting (NP) treatment was less advantageous for nutrient retention, it effectively maintained soil physical structure and water retention capacity.

Table 3 Temporal dynamics of soil quality parameters

Parameter	ΔHP	ΔLP	ΔNP	ΔCK
PH	–0.77±0.17^{b}	–0.51±0.48^{b}	0.87±0.66^{a}	–0.52±0.26^{b}
Alkaline-hydrolyzable N/mg·kg^{-1}	–1.21±39.23^{a}	–35.78±13.18^{ab}	–64.48±47.67^{b}	–83.54±13.05^{b}
Available P/mg·kg^{-1}	25.51±15.24^{a}	–16.67±8.41^{b}	–11.93±6.56^{b}	16.42±6.01^{a}
Available K/mg·kg^{-1}	95.68±58.73^{a}	–9.28±27.75^{ab}	–99.55±22.73^{b}	55.35±92.41^{a}
Total N/mg·g^{-1}	–0.69±0.18^{a}	–1.04±0.17^{ab}	–1.14±0.45^{ab}	–1.53±0.14^{b}
Total P/g·kg^{-1}	1.93±0.23^{a}	1.69±0.31^{a}	0.56±0.68^{b}	1.24±0.03^{ab}
Total K/g·kg^{-1}	6.84±6.41^{a}	5.87±2.88^{a}	4.06±3.97^{a}	12.01±8.77^{a}
EC/μS·cm^{-1}	253.53±262.88^{a}	120.3±90.19^{a}	–77.87±316.78^{a}	20.37±29.44^{a}
Soil organic matter/g·kg^{-1}	–7.42±7.05^{a}	–25.28±3.43^{ab}	–33.89±17.54^{b}	–41.1±10.22^{b}
Soil organic carbon/g·kg^{-1}	–4.31±4.09^{a}	–14.66±1.99^{ab}	–19.66±10.17^{b}	–23.84±5.93^{b}
Water content/%	1.13±1.93^{b}	3.12±1.60^{ab}	5.59±3.06^{a}	–3.68±0.50^{c}
Maximum water holding capacity/g·kg^{-1}	–77.15±92.57^{b}	–107.76±11.23^{b}	147.23±39.20^{a}	–139.11±27.16^{b}
Bulk density/g·cm^{-3}	–0.04±0.08^{ab}	0.01±0.04^{a}	–0.13±0.04^{b}	0.04±0.03^{a}
Porosity/%	–9.3±3.61^{b}	–7.79±3.51^{b}	4.52±3.11^{a}	–7.5±2.22^{b}

3.2 Comprehensive effects of shading intensity on the growth, yield, quality, and antioxidant system of *B. oleracea*

3.2.1 Effects of different shading gradients in the agrivoltaic system on the agronomic traits and yield of *B. oleracea*

The measurements of agronomic traits and yield of *B. oleracea* are presented in Table 4. Different shading gradients significantly influenced the growth indicators of *B. oleracea*. NP performed best across most agronomic traits, with significantly higher head transverse diameter, head vertical diameter, and single head weight than HP and LP (p<0.05). HP and LP showed no significant differences in these traits, and leaf morphology (length and width) was unaffected by shading. Yield followed NP>LP>HP (Table 4).

Table 4 Effects of different shading gradients in the agrivoltaic system on the agronomic traits of *B. oleracea*

Parameter	HP	LP	NP
Plant height/cm	22.93±0.78^{ab}	21.78±1.18^{b}	25.88±4.33^{a}
Head transverse diameter/cm	16.68±2.26^{b}	15.8±1.01^{b}	18.78±0.76^{a}
Head vertical diameter/cm	15.62±1.80^{b}	15.7±0.47^{b}	17.3±0.79^{a}
Number of leaves	12.17±0.98^{ab}	11.33±1.51^{b}	12.83±0.75^{a}
Leaf length/cm	30.02±5.54^{a}	32.53±2.74^{a}	31.65±2.62^{a}
Leaf width/cm	30.32±2.34^{a}	29.92±3.01^{a}	31.17±2.53^{a}
Single head weight/kg	1.23±0.28^{b}	1.25±0.14^{b}	1.79±0.23^{a}
Yield/kg·(4m^{2})$^{-1}$	22.93±2.22^{c}	29.64±1.36^{b}	36.26±4.71^{a}

These results demonstrate that sufficient light conditions favor plant growth and head formation in *B. oleracea*. Plants grown in the unshaded environment showed distinct advantages in plant height, head size, and single head weight. However, shading from the PV panels had little influence on leaf morphology.

3.2.2 Effects of different shading gradients in the agrivoltaic system on the quality of *B. oleracea*

Quality parameters are presented in Table 5. LP exhibited the

best overall quality profile, with significantly higher total sugar, fructose, and starch contents than HP and NP. Sucrose and total polysaccharide contents were significantly higher in HP and LP than in NP. HP promoted the accumulation of structural substances, with the highest cellulose and lignin contents among all treatments. SPAD values in HP and NP were similar and significantly higher than in LP. No significant differences were observed for soluble sugar, reducing sugar, glucose, or hemicellulose (Table 5). These results indicate that low shading favors sugar and starch accumulation, whereas high shading promotes structural substance synthesis, demonstrating the differential regulatory effects of the shading gradient on quality formation in *B. oleracea*.

Table 5 Effects of different shading gradients in the agrivoltaic system on the quality of *B. oleracea*

Parameter	HP	LP	NP
Soluble sugar content/mg·g^{-1}	239.3±22.80^{a}	268.89±36.84^{a}	206.15±50.94^{a}
Reducing sugar content/μg·g^{-1}	62 606.51 ±3341.30^{a}	66 905.54 ±2795.63^{a}	64 361.78 ±4813.64^{a}
Total sugar content/mg·g^{-1}	94.23±9.80^{b}	113.15±5.56^{a}	99.59±2.17^{b}
Sucrose content/mg·g^{-1}	2.29±0.42^{a}	2.15±0.81^{a}	0.94±0.39^{b}
Total polysaccharide content/μg·g^{-1}	2927.59±370.53^{a}	3046.3±232.20^{a}	2140.2±206.85^{b}
Glucose content/μmol·g^{-1}	34.53±2.58^{a}	37.02±2.15^{a}	32.32±2.86^{a}
Fructose content/mg·g^{-1}	131.25±22.78^{b}	201.47±10.24^{a}	129.17±8.63^{b}
Starch content/mg·g^{-1}	6.9±0.31^{b}	8±0.34^{a}	5.94±0.06^{c}
Hemicellulose content/mg·g^{-1}	331.79±19.69^{a}	341.42±15.74^{a}	333.14±32.88^{a}
Cellulose content/mg·g^{-1}	581.43±20.98^{a}	543.62±17.22^{a}	494.89±22.22^{b}
Lignin content/%	15.3±3.56^{a}	7.48±1.85^{b}	8.87±0.75^{b}
Chlorophyll SPAD value	71.73±3.65^{a}	63.73±3.87^{b}	73.47±4.45^{a}

3.2.3 Effects of different shading gradients in the agrivoltaic system on the antioxidant capacity of *B. oleracea*

Antioxidant capacity parameters are presented in Table 6. NP exhibited the highest POD activity and the lowest MDA and H_2O_2 contents, indicating efficient peroxide scavenging and minimal membrane lipid peroxidation under full sunlight. Conversely, HP showed the highest CAT activity. SOD activity did not differ significantly among treatments (Table 6). These results demonstrate that the shading gradient induces differentiated antioxidant strategies in *B. oleracea*: POD plays a dominant role under full sunlight conditions, whereas CAT is preferentially activated under high shading to maintain redox homeostasis.

Table 6 Effects of different shading gradients in the agrivoltaic system on the antioxidant capacity of *B. oleracea*

Parameter	HP	LP	NP
Superoxide Dismutase (SOD) activity/U·g^{-1}	32.64±5.84^{a}	31.68±4.22^{a}	36.89±6.69^{a}
Catalase (CAT) activity/U·g^{-1}	464.08±124.51^{a}	242.3±39.67^{b}	117.99±10.30^{b}
Peroxidase (POD) activity/U·g^{-1}	523.1±54.50^{b}	141.19±21.90^{c}	1832.89±226.31^{a}
Malondialdehyde (MDA) content/nmol·g^{-1}	6.55±0.75^{a}	7.49±0.24^{a}	3.93±1.23^{b}
Hydrogen Peroxide (H_2O_2) content/μmol·g^{-1}	0.39±0.04^{a}	0.36±0.03^{a}	0.22±0.05^{b}

3.3 Identification of key genes and pathways in *B. oleracea* in response to shading stress via transcriptome sequencing

3.3.1 Quality assessment of transcriptome sequencing data

To elucidate the gene expression regulatory mechanisms of *B. oleracea* under different shading gradients, transcriptome sequencing was performed on leaf samples from the HP (high-shading), LP (low-shading), and NP (no-shading) treatments. The sequencing quality control results are summarized in Table 7. The sequencing error rate for all samples was 0.02%. The Q20 and Q30 scores ranged from 99.16% to 99.38% and 96.87% to 97.67%, respectively, and the GC content remained stable between 45.97% and 47.09%. After data filtering, the retention rate of Clean Reads from the Raw Reads was high for all treatments. These metrics indicate excellent sequencing data quality, with base calling accuracy and sequence reliability meeting the requirements for subsequent transcriptomic analyses, including differential expression analysis, functional annotation, and pathway enrichment.

Table 7 Summary of sequencing output and quality metrics

Sample	Group	Raw reads	Clean reads	Error rate/%	Q20/%	Q30/%	GC content/%
HP1	HP	58 918 030	57 906 078	0.02	99.34	97.52	46.21
HP2	HP	50 615 044	49 659 456	0.02	99.28	97.32	46.06
HP3	HP	58 839 908	57 693 560	0.02	99.38	97.67	45.97
LP1	LP	44 837 520	44 172 310	0.02	99.18	96.92	46.8
LP2	LP	54 680 890	53 923 922	0.02	99.18	96.96	46.78
LP3	LP	67 881 802	66 882 420	0.02	99.24	97.15	46.79
NP1	NP	49 314 288	48 698 822	0.02	99.18	96.93	46.89
NP2	NP	48 815 164	48 199 636	0.02	99.16	96.87	47.08
NP3	NP	52 842 850	52 130 930	0.02	99.31	97.4	47.09

The PCA plot is shown in Figure 1. Principal components 1 (PC1) and 2 (PC2) explained 36.2% and 28.1% of the variance, respectively, with a cumulative contribution rate of 64.3%, effectively reflecting the overall expression differences among samples. Regarding sample distribution, the HP, LP, and NP *B. oleracea* samples formed completely distinct clusters in the PCA space: HP samples clustered in the left upper quadrant, LP samples grouped in the right lower quadrant, and NP samples clustered in the right upper quadrant. The replicates within each group showed good cohesion. This result demonstrates that the PV panel shading gradient significantly reshaped the transcriptomic expression profiles of *B. oleracea*, revealing systematic differences in gene expression patterns under varying shading intensities. These data provide foundational evidence of global expression differences for subsequent mining of key genes and regulatory pathways responsive to shading stress.

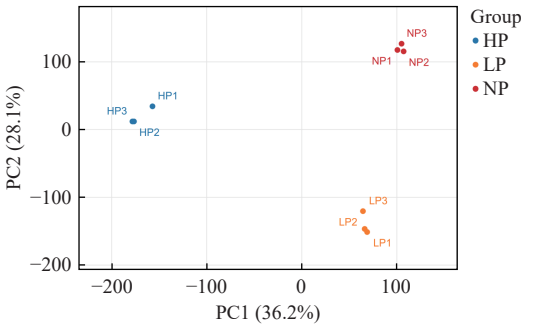

Figure 1 Principal component analysis (PCA) score plot of *B. oleracea* transcriptome samples under different shading gradients

3.3.2 Screening and overall analysis of differentially expressed genes (DEGs)

To decipher the differential patterns of gene expression in *B. oleracea* under varying shading gradients, differentially expressed genes (DEGs) were screened and analyzed across comparisons between the HP (high-shading), LP (low-shading), and NP (no-shading) groups. As shown in Figure 2a, among the three pairwise comparisons (HP vs LP, HP vs NP, and LP vs NP), the HP vs NP comparison yielded the highest number of DEGs. In all

comparisons, the number of up-regulated genes exceeded the number of down-regulated genes, indicating that the transcriptomic differences between high-shading and no-shading conditions were the most pronounced. The Venn diagram (Figure 2b) further revealed 338 overlapping DEGs common to all three comparisons. Simultaneously, a substantial number of unique DEGs were identified in each comparison: 1127 unique to HP vs LP and 995 unique to LP vs NP. This suggests that the differential gene expression in *B. oleracea* under different shading gradients involves both common regulatory modules and specific response mechanisms. The volcano plots in Figures 2c, 2d, and 2e visually represent the distribution of DEGs for each comparison: red dots denote significantly up-regulated genes, blue dots signify significantly down-regulated genes, and grey dots represent genes with no significant difference. In the HP vs LP (Figure 2c), HP vs NP (Figure 2d), and LP vs NP (Figure 2e) comparisons, the significantly differentially expressed genes were markedly enriched on both sides of the plots, with up-regulated genes consistently outnumbering down-regulated ones. This further validates the significant differences in gene expression in *B. oleracea* subjected to different shading treatments. In summary, the PV panel shading gradient drives an adaptive transcriptomic response in *B. oleracea* by regulating the differential expression of a large number of genes, laying a foundation for subsequent functional gene mining and pathway analysis.

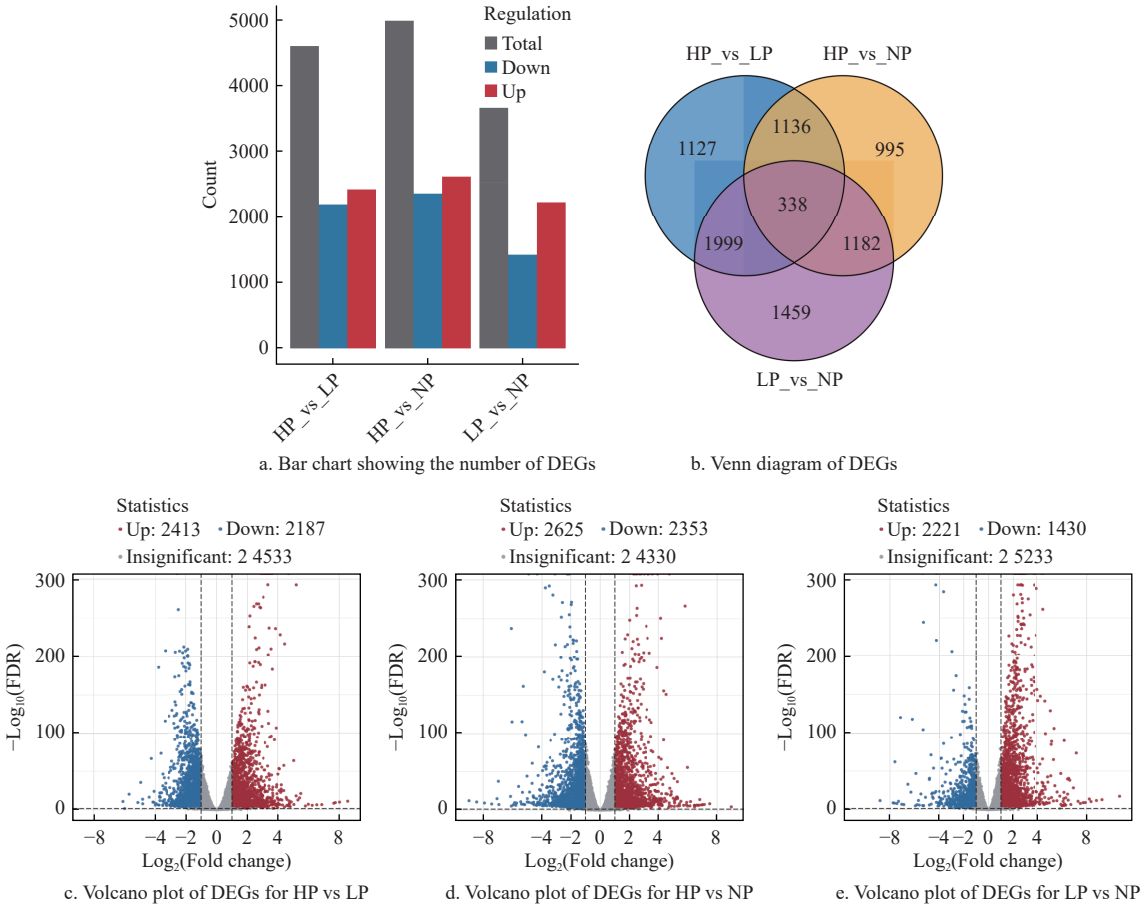

a. Bar chart showing the number of DEGs b. Venn diagram of DEGs

c. Volcano plot of DEGs for HP vs LP d. Volcano plot of DEGs for HP vs NP e. Volcano plot of DEGs for LP vs NP

Figure 2 Analysis of differentially expressed genes (DEGs) in *B. oleracea* under different shading gradients

3.3.3 Functional and pathway enrichment analysis of differentially expressed genes

To further investigate the functions and regulatory pathways of the differentially expressed genes (DEGs), Gene Ontology (GO) functional enrichment and Kyoto Encyclopedia of Genes and Genomes (KEGG) pathway enrichment analyses were performed, with the results shown in Figure 3.

GO enrichment analysis (Figure 3a) revealed that photosynthesis-related terms, including "photosynthesis," "light harvesting," "photosystem I/II," and "chlorophyll binding," were significantly enriched across all three comparisons, indicating that shading intensity substantially remodeled the photosynthetic gene regulatory network. KEGG pathway analysis (Figure 3b) identified "Metabolic pathways," "Biosynthesis of secondary metabolites," "Photosynthesis," "Photosynthesis-antenna proteins," "Carbon fixation in photosynthetic organisms," "Starch and sucrose metabolism," and "Plant hormone signal transduction" as the most significantly enriched pathways across comparisons. These results indicate that shading stress triggers a multi-layered transcriptomic response in *B. oleracea*, centered on photosynthetic carbon metabolism and coordinated with hormone signaling.

3.3.4 Screening of key genes and co-expression network analysis

To systematically decipher the molecular mechanisms underlying the adaptation of *B. oleracea* to light shading stress within the agrivoltaic system, core regulatory genes were identified by applying stringent differential expression criteria (FDR<0.05 and $|\log_2\text{FoldChange}|\geq 1$) and integrating gene functional annotations with KEGG pathway information. As shown in Table 8, these genes exhibited significant expression changes along the gradient from the no-shading (NP) zone to the low-shading (LP) and high-shading (HP) zones, and were precisely enriched in a series of key biological pathways.

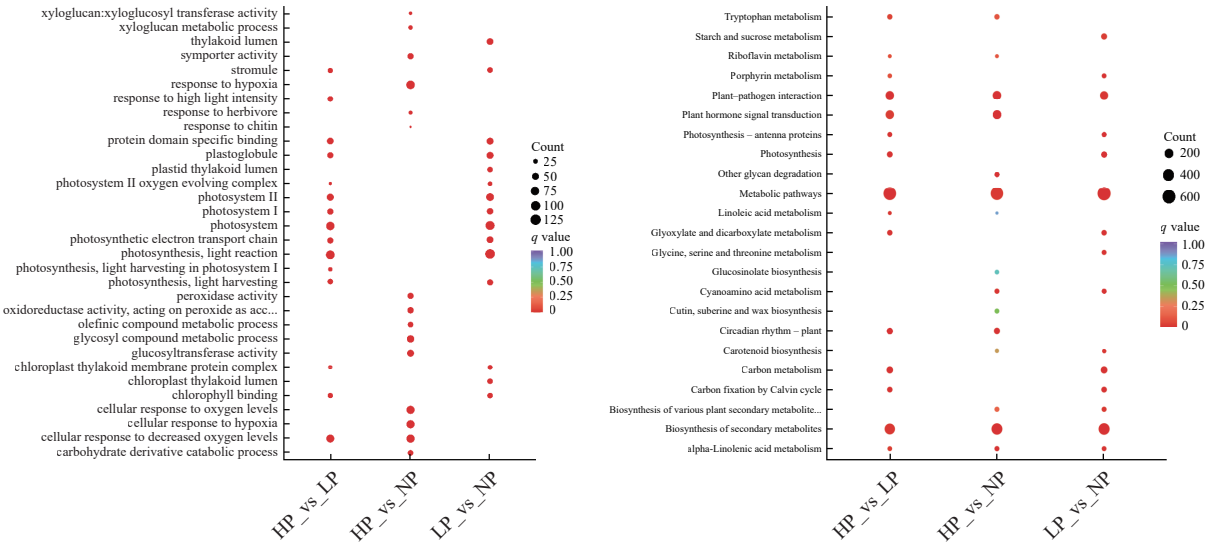

a. Bubble plot of GO functional enrichment b. Bubble plot of KEGG pathway enrichment

Figure 3 GO functional enrichment and KEGG pathway enrichment analysis of differentially expressed genes (DEGs) in *B. oleracea* under different shading gradients

Table 8 Screening and functional characterization of key differentially expressed genes in *B. oleracea* under different shading conditions

Gene ID	HP vs NP log2FC, (*p*-value)	LP vs NP log2FC, (*p*-value)	HP vs LP log2FC, (*p*-value)	KEGG pathway	Description
Bo3g090010	5.82 (p=4.37e^{-270})	0.66(p=0.029)	5.21(p=8.44e-^{302})	Not annotated	Uncharacterized protein LOC106331916
Bo1g007330	–2.23(p<2.2e^{-16})	0.38(p=1.04e^{-14})	–2.44(p<2.2e^{-16})	Not annotated	Ethylene-responsive transcription factor ERF109 isoform X1
Bo4g182560	0.48 (p=6.40e^{-17})	2.37(p<2.2e^{-16})	–1.85(p=7.88e^{-195})	Photosynthesis - antenna proteins; Metabolic pathways	Chlorophyll a-b binding protein 1, chloroplastic-like
Bo3g039200	1.87(p=5.20e^{-233})	–1.43(p=1.09e^{-111})	3.34(p<2.2e^{-16})	Plant hormone signal transduction	Jasmonic acid-amido synthetase JAR1-like
Bo1g007900	–5.36(p=1.58e^{-118})	–7.14(p=3.86e^{-123})	1.83(p=2.93e^{-07})	MAPK signaling pathway - plant; Plant hormone signal transduction; Plant-pathogen interaction	Pathogenesis-related protein 1
Bo3g146480	2.27(p<2.2e^{-16})	2.80(p<2.2e^{-16})	–0.48(p=6.73e^{-12})	Photosynthesis - antenna proteins; Metabolic pathways	Chlorophyll a-b binding Protein 1, chloroplastic
Bo1g150250	2.53(p=1.01e^{-20})	0.29(p=0.629)	2.29(p=9.99e^{-05})	Not annotated	Hydrophobic protein RCI2B
Bo3g027740	0.74(p = 3.78e^{-40})	2.55(p<2.2e-^{16})	–1.76(p=6.20e^{-194})	Photosynthesis - antenna proteins; Metabolic pathways	Chlorophyll a-b binding protein 1, chloroplastic
Bo6g079880	1.43(p=7.18e^{-154})	2.62(p<2.2e^{-16})	–1.14(p=1.28e^{-81})	Linoleic acid metabolism; alpha-Linolenic acid metabolism; Metabolic pathways; Biosynthesis of secondary metabolites	Lipoxygenase 2, chloroplastic-like
Bo2g028580	–5.28(p=4.88e^{-165})	–6.19(p=6.79e^{-121})	1.28(p=NA)	Phenylpropanoid biosynthesis; Metabolic pathways; Biosynthesis of secondary metabolites	Peroxidase 67-like

Note: *p*-values listed as <2.2e^{-16} exceed computational precision. For the gene Bo2g028580 in the HP vs LP comparison, a *p*-value was not available (NA) from the differential expression analysis pipeline, though a fold change was calculated. The absence of KEGG pathway annotation for some genes is common and does not affect the main conclusions.

The remodeling of photosynthesis-related gene expression was particularly notable. Several genes encoding chlorophyll a/b binding proteins, including Bo3g146480, Bo3g027740, and Bo4g182560, were enriched in the "Photosynthesis - antenna proteins" pathway. Among them, the expression pattern of Bo4g182560 revealed a fine distinction in the plant's response to shading intensity: its expression was significantly up-regulated under low shading compared to normal light conditions (LP vs NP, $\log_2$FC=2.37, p<2.2e^{-16}), whereas it was markedly down-regulated in high shading compared to low shading (HP vs LP, $\log_2$FC=–1.85, p=7.88e^{-195}). This dynamic change suggests that under mild shading, *B. oleracea* enhances its light-harvesting capacity to maintain energy supply; however, as shading intensifies, it likely initiates strategic adjustments, reducing resource investment in photosynthetic apparatus.

Beyond direct photosynthetic regulation, shading stress also triggered complex hormonal and metabolic reprogramming. The expression of Bo3g039200, a key gene in the jasmonic acid signaling pathway (a homolog of jasmonic acid-amido synthetase JAR1), increased sharply in the comparison between high and low shading (HP vs LP, $\log_2$FC=3.34, p<2.2×10^{-16}), highlighting the central role of jasmonic acid in mediating the response to severe shading. Concurrently, the significant up-regulation of Bo6g079880 (lipoxygenase 2) under shading conditions (LP vs NP, $\log_2$FC=2.62, p<2.2e^{-16}) linked it closely to pathways such as "Linoleic acid metabolism" and "alpha-Linolenic acid metabolism," indicating that oxylipins and their derived signaling molecules (e.g., JA precursors) collectively form an early metabolic signaling network responding to light stress.

Furthermore, this study uncovered other important stress response mechanisms. For instance, the expression of Bo1g007900 (pathogenesis-related protein PR1) was strongly suppressed under shading (HP vs NP, $\log_2$FC=–5.36, p=1.58e^{-118}), reflecting that plants facing abiotic stress might reallocate energy resources by

down-regulating parts of the biotic stress defense pathways. Notably, a gene of unknown function, Bo3g090010, exhibited extremely significant expression changes (HP vs NP, $\log_2$FC=5.82, p=4.37e^{-270}). Its specific activation under high shading strongly suggests its potential role as a key factor involved in shade perception or early signal transduction, warranting further investigation.

In summary, the key genes screened in this study collectively outline a multi-layered transcriptional regulatory blueprint for the response of *B. oleracea* to shading stress. This network encompasses multiple levels, from light signal perception and photosynthetic apparatus adjustment to hormone signal transduction and global metabolic reorganization, systematically revealing the molecular basis for the transcriptome-level adaptation of *B. oleracea* to the changing light environment in the agrivoltaic system. This provides important candidate targets and a theoretical basis for improving shade tolerance in crops.

3.3.5 qRT-PCR validation of key differentially expressed genes

To independently verify the reliability of the transcriptome sequencing results, this study employed quantitative real-time PCR (qRT-PCR) to analyze the expression patterns of 10 previously screened key differentially expressed genes (DEGs) under the different shading conditions of the agrivoltaic system (Figure 4).

The results indicated that the qRT-PCR expression trends for the vast majority of genes were highly consistent with the transcriptome data. This included Bo3g027740, Bo3g039200, Bo3g146480, Bo4g182560, Bo2g028580, Bo1g007900, and Bo6g079880. This finding strongly confirms the accuracy of the RNA-seq data in this study. However, discrepancies in expression patterns between the two platforms were observed for three genes (Bo1g007330, Bo1g150250, Bo3g090010). Such inconsistencies may stem from various factors, such as post-transcriptional regulation affecting the correlation between transcript levels and final functional protein levels, or inherent technical characteristics of the methods, including their different dynamic detection ranges and sensitivities. Nevertheless, the high validation rate (70%) for the key genes provides a reliable experimental basis for subsequent in-depth research into the molecular mechanisms by which these genes regulate the light adaptability of *B. oleracea* in the agrivoltaic system.

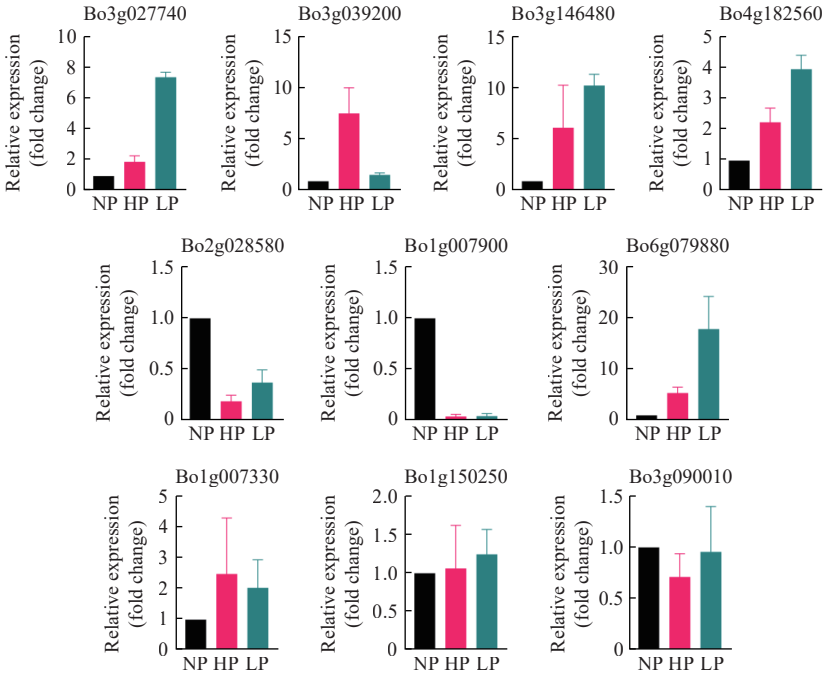

Relative expression levels were calculated using the $2^{(-\Delta\Delta Ct)}$ method with Actin as the internal reference. Data are presented as mean±SD (n=3 technical replicates).

Figure 4 qRT-PCR validation of RNA-seq results for 10 selected DEGs in *B. oleracea* under NP, HP, and LP treatments

4 Discussion

4.1 Trade-off mechanisms in growth and resource allocation of *B. oleracea* under shading gradients

This study demonstrates that the shading gradient within the agrivoltaic system profoundly influenced the resource allocation strategy of *B. oleracea*. The high-shading (HP) environment, while favorable for maintaining soil moisture and nutrient contents such as alkaline-hydrolyzable nitrogen, available phosphorus, and available potassium, severely limited photosynthesis, resulting in the lowest biomass accumulation. As a compensatory mechanism, *B. oleracea* allocated a greater proportion of photoassimilates to structural tissues, manifested as significantly increased cellulose and lignin contents. In contrast, the no-shading (NP) condition provided ample energy for photosynthetic carbon accumulation, driving the allocation of assimilates towards harvested organs and thereby achieving the highest yield. The low-shading (LP) condition exhibited an ideal balanced state, maintaining a yield close to that of the NP zone while its specific light environment potentially optimized carbon metabolic flux, promoting the accumulation of quality components such as sugars and starch.

Crop responses to photovoltaic shading exhibit significant species specificity. For instance, in greenhouse cultivation of chili pepper (*Capsicum annuum* cv. Omega), photovoltaic shading did not significantly affect plant growth or final yield but significantly reduced fruit vitamin C content and promoted earlier flowering and an extended shelf life[52]. This result contrasts sharply with the quality improvement observed in the LP zone for *B. oleracea* in this study, indicating that the effects of shading on crop physiology and metabolism are species-dependent. This also suggests that the configuration of cropping systems within agrivoltaic systems requires comprehensive consideration of crop light adaptability and

quality formation patterns.

Furthermore, the patterns observed in this study in a subtropical humid mountainous region present interesting similarities and differences with reports on photovoltaic shading in arid ecosystems. Research in arid zones indicates that PV panel shading can aid soil organic carbon accumulation and alter plant biomass allocation patterns[53], which aligns with the enhanced soil nutrient retention capacity and structural substance accumulation observed in the HP zone of this study. This suggests a potential cross-ecosystem universality of photovoltaic shading in regulating the "soil-plant" carbon allocation relationship. However, unlike the common risks of biomass decline and impaired microbial activity reported in arid zones, the LP zone in this system significantly enhanced quality while maintaining yield, with relatively well-preserved soil fertility. This difference highlights the critical role of ecosystem water conditions in modulating the comprehensive benefits of agrivoltaic systems: in water-sufficient regions, moderate shading may not constitute a stress but rather, through microclimate optimization, become an opportunity for quality enhancement.

It is worth emphasizing that the CK (high-shading, no plant) treatment established in this experiment provided a crucial entry point for dissecting the interaction between the "shading environmental effect" and "crop biological feedback." Data indicate that the shaded micro-environment itself indeed constitutes a "soil nutrient reservoir," but the introduction of crops fundamentally altered the system's trajectory. In the HP zone, *B. oleracea* essentially faced a physiological dilemma: its root system resided in a soil environment relatively "rich in nitrogen," while its shoots suffered from severe "carbon starvation" due to insufficient light intensity. This systemic imbalance in carbon-nitrogen resources prevented the crop from effectively utilizing sufficient nitrogen for growth-related synthesis. Instead, driven by the abundant nitrogen availability, the relatively surplus carbon skeletons were disproportionately channeled towards the synthesis of cell wall structural components, such as lignin and cellulose. This quantitative relationship reveals that under intense shading, nutrient "availability" does not equate to crop "utilizability," and the capacity for carbon assimilation becomes the key bottleneck determining nutrient flow and crop performance. Consequently, the final performance of crops in agrivoltaic systems is not determined solely by either soil or light factors individually, but rather by the integrated efficiency of carbon and nutrient utilization at the physiological level within the plant. This understanding holds core guiding significance for directing varietal selection and the precise management of carbon and nitrogen resources in agrivoltaic systems.

4.2 Multidimensional physiological responses and molecular regulatory network of *B. oleracea* under photovoltaic shading

4.2.1 Trade-off strategies in photosynthetic carbon acquisition and their molecular basis

Deep integration of transcriptomic and phenotypic data revealed that the photosynthetic regulatory strategies employed by *B. oleracea* in response to shading are highly environment-specific. The significant up-regulation of the chlorophyll a/b binding protein gene Bo4g182560 under LP vs NP ($log_2FC=2.37$) indicates that under mild shading, *B. oleracea* implements an "efficiency compensation" strategy to maximize light capture. This allowed it to significantly increase total sugar and starch content while incurring only an 18.26% yield loss. Conversely, the significant down-regulation of this gene under HP vs LP ($log_2FC=-1.85$) suggests that under deep shading, the plant switches to a "resource conservation" strategy, reducing investment in potentially inefficient photosynthetic apparatus, which directly contributed to the lowest yield in the HP zone.

A key finding was that chlorophyll content (SPAD) was similar in HP and NP and significantly higher than in LP, whereas the chlorophyll a/b-binding protein gene Bo4g182560 was most highly expressed in LP. This physiological-transcriptional discrepancy likely reflects an optimized resource allocation strategy under mild shading: *B. oleracea* up-regulates light-harvesting complex genes to maximize light capture efficiency while moderately suppressing bulk chlorophyll biosynthesis to conserve nitrogen and metabolic resources, thereby prioritizing the adjustment of photosynthetic machinery and the formation of yield and quality components. This interpretation is supported by previous research showing that phytochrome A (PHYA) plays a crucial role in fine-tuning chlorophyll biosynthesis under partial shading, helping leaves optimize their photosynthetic apparatus for low light and maintain carbon balance rather than directly inducing senescence[54]. Thus, the lower chlorophyll content in LP is not indicative of functional decline, but rather represents an active physiological adaptation orchestrated by the light signaling system.

4.2.2 Environment-specific division of labor in the antioxidant enzyme system

From gene to phenotype, different shading environments shaped distinct antioxidant defense patterns in *B. oleracea*. In the NP zone, the high-light environment induced significant oxidative stress. The high expression of the peroxidase gene Bo2g028580 and its corresponding extremely high POD enzyme activity (1832.89 U/g, Table 6) constituted an efficient scavenging system to cope with the large amount of peroxides produced during photo-oxidation. This resulted in the lowest MDA content (3.93 μmol/g), indicating the least membrane lipid peroxidation damage. In contrast, in the HP zone, although light intensity was reduced, the shading environment might have induced hydrogen peroxide (H_2O_2) accumulation in specific cellular compartments (e.g., peroxisomes) by altering metabolic pathways (e.g., photorespiration or fatty acid β-oxidation). To address this, *B. oleracea* significantly enhanced catalase (CAT) activity (464.08 U/g) to directly and efficiently catalyze the decomposition of H_2O_2, thereby maintaining cellular redox homeostasis.

This phenomenon of shading-induced remodeling of the plant antioxidant system appears universal. For instance, strawberries cultivated under semi-transparent PV panels showed significantly higher fruit total phenol content and free radical scavenging activity compared to the unshaded control[55]. This finding complements this study: strawberries employ chemical scavenging by accumulating phenolic secondary metabolites, whereas *B. oleracea* utilizes enzymatic scavenging by regulating core antioxidant enzymes (POD and CAT). Although the mechanisms differ, both findings confirm that shading, as a key environmental signal, can systematically trigger specific antioxidant metabolic pathways in plants. In summary, the precise division of labor—relying on POD in the NP zone to counter photo-oxidation and on CAT in the HP zone to alleviate peroxide stress—constitutes a core physiological mechanism for *B. oleracea* to adapt to different light environments.

4.2.3 JA signaling pathway mediates growth-defense balance and quality regulation

The jasmonic acid (JA) signaling pathway exhibited a tiered regulatory characteristic in *B. oleracea* responding to different shading intensities, playing a central role, particularly in coordinating the growth-defense balance. The significant increase in

expression of the jasmonic acid-amido synthetase gene Bo3g039200 (JAR1) under HP vs LP (log_2FC=3.34, Table 8) indicates its specific activation under severe shading, subsequently pushing the plant into a comprehensive defense state. Notably, the expression pattern of the lipoxygenase gene Bo6g079880 (LOX2) was not entirely synchronized with JAR1; its expression was highest in the LP zone, intermediate in HP, and lowest in NP, suggesting a certain degree of decoupling between JA synthesis and signaling components under the shading gradient.

This expression divergence suggests that under mild shading (LP) conditions, LOX2 might be involved in pre-adapting carbon metabolism and optimizing quality components by modulating lipid signaling pathways. In contrast, under severe shading (HP) conditions, the strong induction of JAR1 initiates a stress response program primarily characterized by growth inhibition and enhanced structural defense. This result aligns with the findings of Yang et al.[56], concluding that under severe shading stress, plants up-regulate JA signaling to prioritize defense activation, thereby sacrificing part of their growth potential for basic survival. The significantly increased lignin content in the HP zone is a direct manifestation of this strategy.

Simultaneously, the high-sugar and high-starch quality advantages observed in the LP zone correspond with the significant enrichment of the "starch and sucrose metabolism" pathway in the transcriptome, further indicating that mild shading optimizes the storage form and accumulation efficiency of photosynthetic products by directionally regulating the expression of carbon metabolism-related genes.

4.3 General discussion, study limitations, and application prospects

By integrating a multidimensional evidence chain encompassing soil properties, plant physiology, and transcriptomics, this study systematically elucidates the growth trade-off mechanisms and molecular regulatory network of *B. oleracea* under shading gradients. The core finding is that *B. oleracea* exhibits a precise environmental adaptation within the agrivoltaic system: high shading (HP) induces a "defense-priority" strategy centered on jasmonic acid signaling, accompanied by the allocation of carbon resources towards structural substances; low shading (LP) significantly enhances quality while maintaining high yield by optimizing photosynthetic antenna and carbon metabolism pathways; whereas no shading (NP) maximizes biomass accumulation. This cascade response model of "soil-light environment-crop" interactions deepens the understanding of crop adaptation mechanisms in such integrated systems.

It is important to note that crop responses to photovoltaic shading are complex and diverse. A recent study on soybeans indicated that semi-transparent PV panels, due to their ability to maintain a more favorable light environment, had the least negative impact on crop nitrogen accumulation and protein content[57]. This finding resonates with the superiority of the LP zone observed in this study, collectively suggesting that optimizing the light environment is an effective approach to safeguarding crop productivity in agrivoltaic systems. However, this research further reveals that even the severe shading environment represented by HP is not merely an "ecological adversity" but rather induces a unique survival strategy characterized by defense and structural reinforcement. Therefore, future research should not stop at seeking an "optimal" shading degree but should delve deeper into analyzing the specific physiological and molecular mechanisms shaped by different shading environments. This will provide a precise theoretical basis for the differential utilization of various zones and for maximizing the system's comprehensive benefits.

Several limitations should be acknowledged. First, shading rates were estimated geometrically based on PV array configuration rather than measured continuously with PAR sensors, which may not fully capture diurnal and seasonal variations in actual light distribution at the canopy level. Second, transcriptomic profiling was performed only at harvest; temporal dynamics of gene expression across the growing season remain unexplored, limiting the understanding of when key regulatory pathways such as photosynthesis, starch and sucrose metabolism, and hormone signaling are activated under different shading conditions. Third, only a single cultivar ("Xiaotietou") was tested, and since shade tolerance varies among genotypes, the generalizability of the antioxidant strategy differentiation and quality responses observed here to other *B. oleracea* cultivars requires further evaluation. Fourth, the candidate genes identified, including Bo3g090010 and Bo4g182560, await functional validation through reverse genetics. Finally, this study did not examine the soil microbial community; integrating microbial data would help construct a more complete "PV panel-soil-microbe-crop" interaction network.

Based on the above understanding, the optimal management of agrivoltaic systems should be grounded in the precision agriculture concept of "zonal management". The LP zone, with its suitable light and temperature conditions, can serve as a production area for high-quality agricultural products, focusing on high-quality fruits and vegetables. Although the HP zone is unfavorable for high yields of conventional crops, its cool and humid microclimate can be utilized as a production area for shade-tolerant specialty crops or an ecological conservation zone. The NP zone should function as the high-yield core area, dedicated to maximizing grain production. To realize this blueprint, future management practices must rely on environmental sensors, remote sensing monitoring, and intelligent decision-support systems to implement differentiated irrigation, fertilization, and crop configuration for different zones. Ultimately, this will advance agrivoltaic systems from simple "space sharing" towards "functional synergy" based on precise niche identification, thereby achieving a win-win situation for energy, food, and ecological benefits.

5 Conclusions

This study, through the integration of multidimensional data encompassing soil physicochemical properties, plant physiology, and transcriptomics, systematically reveals the multifaceted mechanisms by which shading gradients govern the growth of *B. oleracea* in an agrivoltaic system. The principal conclusions are as follows:

1) The shading gradient significantly regulated the growth and resource allocation of *B. oleracea*. The NP condition maximized biomass and yield. The LP condition significantly enhanced sugars and starch while maintaining relatively high yield, which was associated with the up-regulation of photosynthesis-antenna protein genes such as Bo4g182560 and the enrichment of starch and sucrose metabolism. The HP condition limited yield but promoted the synthesis of structural substances (cellulose, lignin), linked to jasmonic acid signaling activation (e.g., Bo3g039200) and a shift in carbon allocation toward secondary cell wall synthesis.

2) The soil environment response exhibited an interaction effect between shading and cultivation. The HP zone maintained higher levels of alkaline-hydrolyzable nitrogen, available phosphorus, and organic matter after the cropping season, demonstrating superior

nutrient retention. In contrast, the NP zone showed significant improvement in physical structure (water holding capacity, porosity).

3) The antioxidant system exhibited environment-specific responses underpinned by distinct transcriptional regulation. The NP zone relied on elevated POD activity to manage oxidative pressure under full sunlight, whereas the HP zone maintained redox homeostasis primarily through enhanced CAT activity. These enzymatic shifts were accompanied by corresponding changes in the expression of antioxidant-related genes, indicating that *B. oleracea* adopts differentiated antioxidant strategies at both the enzymatic and transcriptional levels to adapt to contrasting light environments.

In summary, the shading gradient in the agrivoltaic system collectively shaped the growth performance and adaptive responses of *B. oleracea* through a multi-level "soil-plant-molecular" regulatory network. This study provides a theoretical basis and genetic resources for optimizing crop configuration and precision management in agrivoltaic systems, and establishes a scientific foundation for achieving synergistic efficiency enhancement in the "light-soil-crop" system.

Data availability statement

The transcriptome sequencing data generated in this study have been deposited in the Genome Sequence Archive (GSA) at the National Genomics Data Center (CNCB/Nucleic Acids Research, 2025) under accession number CRA034435 (submission number: subCRA056444). The data are associated with BioProject PRJCA052485 and are publicly accessible at https://ngdc.cncb.ac.cn/gsa. All other supporting data, including soil physicochemical properties, agronomic traits, and physiological indicators, are available within this article and its supplementary materials.

Acknowledgements

This work was supported by the following funding sources:

The Agrivoltaic Systems Technology Research Program of Weining Energy Company (Grant No. 138034FW0420240140), provided by the State Power Investment Corporation Guizhou Jinyuan Weining Energy Co., Ltd.

The Outstanding Young Scientific and Technological Talent Program of Guizhou Province (Grant No. YQK[2023]025), provided by the Department of Science and Technology of Guizhou Province.

Guizhou Vegetable Industry Technology System (Grant No. GZSCCYJSTX), provided by the Department of Agriculture and Rural Affairs of Guizhou Province.

We thank all the above-mentioned institutions for their support.

[References]

[1] Tesfaye B, Lengoiboni M, Zevenbergen J, Simane B. A holistic analysis of food security situation of households engaged in land certification and sustainable land management programs: South Wello, Ethiopia. Foods, 2023; 12(18): 3341.

[2] Fernandez M I, Go Y I, Wong D M L, Früh W G. Review of challenges and key enablers in energy systems towards net zero target: Renewables, storage, buildings, & grid technologies. Heliyon, 2024; 10(23): e40691.

[3] Wang Y J, Wang R, Tanaka K, Ciais P, Penuelas J, Balkanski Y, et al. Global spatiotemporal optimization of photovoltaic and wind power to achieve the Paris Agreement targets. Nat Commun, 2025; 16(1): 2127.

[4] Coşgun A E, Endiz M S, Demir H, Özcan M. Agrivoltaic systems for sustainable energy and agriculture integration in Turkey. Heliyon, 2024; 10(11): e32300.

[5] Goetzberger A, Zastrow A. Kartoffeln unter dem Kollektor. Sonnenenergie, 1981; 3(3): 19–22.

[6] Tan Y, Liu J, Li W D, Yin J H, Chen H, Peng Y T, et al. Agrivoltaics development progresses: From the perspective of photovoltaic impact on crops, soil ecology and climate. Environ Res, 2025; 266: 120540.

[7] Cuppari R I, Branscomb A, Graham M, Negash F, Smith A K, Proctor K, et al. Agrivoltaics: Synergies and trade-offs in achieving the sustainable development goals at the global and local scale. App.Energy, 2024; 362: 122970.

[8] Mäkinen A, Ishihara H, Poque S, Sipari N, Himanen K, Varjus I, et al. Photosynthetic adjustments maintain lettuce growth under dynamically changing lighting in controlled indoor farming setups. Physiol Plant, 2025; 177(4): e70405.

[9] Hickey T, Uchanski M, Bousselot J. Vegetable crop growth under photovoltaic (PV) modules of varying transparencies. Heliyon, 2024; 10(16): e36058.

[10] Ukwu U N, Muller O, Meier-Grüll M, Uguru M I. Agrivoltaics shading enhanced the microclimate, photosynthesis, growth and yields of vigna radiata genotypes in tropical Nigeria. Sci Rep, 2025; 15(1): 1190.

[11] Disciglio G, Stasi A, Tarantino A, Frabboni L. Microclimate modification, evapotranspiration, growth and essential oil yield of six medicinal plants cultivated beneath a dynamic agrivoltaic system in Southern Italy. Plants, 2025; 14(15): 2428.

[12] Zheng J, Meng S D, Zhang X Y, Zhao H L, Ning X L, Chen F C, et al. Increasing the comprehensive economic benefits of farmland with Even-lighting Agrivoltaic Systems. PLoS ONE, 2021; 16(7): e0254482.

[13] Siggers J A, Sturchio M A, Gordon L, Mead S, Smith M D, Knapp A K. Environmental heterogeneity imposed by photovoltaic array alters grassland soil microbial communities. Glob Chang Biol, 2025; 31(7): e70376.

[14] Li X R, Yu Q Q, Yao Z X, Li S, Ma L C, Su K L, et al. The combination of physiological and transcriptomic approaches reveals new insights into the molecular mechanisms of leymus chinensis growth under different shading intensities. Int J Mol Sci, 2025; 26(6): 2730.

[15] Jing X J, Chen P R, Jin X J, Lei J, Wang L J, Chai S S, et al. Physiological, photosynthetic, and transcriptomics insights into the influence of shading on leafy sweet potato. Genes, 2023; 14(12): 2112.

[16] Markin L, Bobrik L. Geometric method for estimating shading degree of objects in solar industry. In: Proceedings of the 31st International Conference on Computer Graphics and Vision (GraphiCon 2021). 2021; pp.645–655. doi: 10.20948/graphicon-2021-3027-645-655.

[17] Bremner J M. Nitrogen—total. In: Sparks D L, Page A L, Helmke P A, Loeppert R H, Soltanpour P N, editors. Methods of soil analysis: Part 3—Chemical methods. Madison: Soil Science Society of America and American Society of Agronomy. 1996; pp.1085–1121.

[18] Roberts P, Stockdale E A, Shepherd M A. Alkaline hydrolysis diffusion method for soil available nitrogen determination. Soil Biol Biochem, 2009; 41(6): 1320–1327.

[19] Bray R H, Kurtz L T. Determination of total, organic, and available forms of phosphorus in soils. Soil Sci, 1945; 59(1): 39–45.

[20] Olsen S R, Sommers L E. Phosphorus. In: Page A L, Miller R H, Keeney D R, editors. Methods of soil analysis: Part 2—Chemical and microbiological properties. Madison: American Society of Agronomy and Soil Science Society of America. 1982; pp.403–430.

[21] Knudsen D, Peterson G A, Pratt P F. Lithium, sodium, and potassium. In: Page A L, Miller R H, Keeney D R, editors. Methods of soil analysis: Part 2—Chemical and microbiological properties. Madison: American Society of Agronomy and Soil Science Society of America. 1982; pp.225–246.

[22] Helmke P A, Sparks D L. Lithium, sodium, potassium, rubidium, and cesium. In: Sparks D L, Page A L, Helmke P A, Loeppert R H, Soltanpour P N, Tabatabai M A, et al. editors. Methods of soil analysis: Part 3—Chemical methods. Madison: Soil Science Society of America and American Society of Agronomy, 1996; pp.551–574.

[23] Mirzakhaninafchi H, Mani I, Hasan M, Nafchi A M, Parray R A, Kumar D. Development of prediction models for soil nitrogen management based on electrical conductivity and moisture content. Sensors, 2022; 22(18): 6728.

[24] McLean E O. Soil pH and lime requirement. In: Page A L, Miller R H, Keeney D R, editors. Methods of soil analysis: Part 2—Chemical and microbiological properties. Madison: American Society of Agronomy and Soil Science Society of America. 1982; pp.199–224.

[25] Nelson D W, Sommers L E. Total carbon, organic carbon, and organic matter. In: Sparks D L, Page A L, Helmke P A, Loeppert R H, Soltanpour

P N, Tabatabai M A, et al. editors. Methods of soil analysis: Part 3—Chemical methods. Madison: Soil Science Society of America and American Society of Agronomy, 1996; pp.961–1010.

[26] Blake G R, Hartge K H. Bulk density. In: Klute A, editor. Methods of soil analysis: Part 1—Physical and mineralogical methods. Madison: American Society of Agronomy and Soil Science Society of America. 1986; pp.363–375.

[27] Gardner W H. Water content. In: Klute A, editor. Methods of soil analysis: Part 1—Physical and mineralogical methods. Madison: American Society of Agronomy and Soil Science Society of America. 1986; pp.493–544.

[28] Yemm E W, Willis A J. The estimation of carbohydrates in plant extracts by anthrone. Biochem J, 1954; 57: 508–514.

[29] Miller G L. Use of dinitrosalicylic acid reagent for determination of reducing sugar. Anal Chem, 1959; 31: 426–428.

[30] Chow P S, Landhäusser S M. A method for routine measurements of total sugar and starch content in woody plant tissues. Tree Physiol, 2004; 24: 1129–1136.

[31] Li W T, Huang D J, Wang B, Hou X M, Zhang R, Yan M, et al. Changes of starch and sucrose content and related gene expression during the growth and development of Lanzhou lily bulb. PLoS ONE, 2022; 17(1): e0262506.

[32] Dubois M, Gilles K A, Hamilton J K, Rebers P A, Smith F. Colorimetric method for determination of sugars and related substances. Anal Chem, 1956; 28: 350–356.

[33] Trinder P. Determination of glucose in blood using glucose oxidase with an alternative oxygen acceptor. Ann Clin Biochem, 1969; 6: 24–31.

[34] Zhang Y, Li X, Wang H. Determination of fructose and glucose in tomato by HPLC with evaporative light-scattering detection. J Sci Food Agric, 2020; 100: 1234–1240.

[35] Tan C T, Zhang L, Duan X W, Chai X R, Huang R M, Kang Y Y, et al. Effects of exogenous sucrose and selenium on plant growth, quality, and sugar metabolism of pea sprouts. J Sci Food Agric, 2022; 102(7): 2855–2863.

[36] Zhang W T, Xu S J, Gao M, Peng S J, Chen L Y, Lao F, et al. Profiling the water soluble pectin in clear red raspberry (*Rubus idaeus L.* cv. Heritage) juice: Impact of high hydrostatic pressure and high-temperature short-time processing on the pectin properties. Food Hydrocoll, 2021; 125: 107439.

[37] Caruso G, Gomez L D, Ferriello F, Andolfi A, Borgonuovo C, Evidente A, et al. Exploring tomato Solanum pennellii introgression lines for residual biomass and enzymatic digestibility traits. BMC Genet, 2016; 17: 56.

[38] Giannopolitis C N, Ries S K. Superoxide dismutases: I. Occurrence in higher plants. Plant Physiology, 1977; 59(2): 309–314.

[39] Hadwan M H. Simple spectrophotometric assay for measuring catalase activity in biological tissues. BMC Biochemistry, 2018; 19: 7.

[40] Chance B, Maehly A C. Assay of catalases and peroxidases. Methods in Enzymology, 1955; 2: 764–775.

[41] Aguilar Diaz De Leon J, Borges C R. Evaluation of oxidative stress in biological samples using the thiobarbituric acid reactive substances assay. Journal of Visualized Experiments, 2020;(159). doi:10.3791/61122.

[42] Velikova V, Yordanov I, Edreva A. Oxidative stress and some antioxidant systems in acid rain-treated bean plants: protective role of exogenous polyamines. Plant Science, 2000; 151(1): 59–66.

[43] Chen S, Zhou Y, Chen Y, Gu J. fastp: an ultra-fast all-in-one FASTQ preprocessor. Bioinformatics, 2018; 34(17): i884–i890.

[44] Pertea M, Pertea G M, Antonescu C M, Chang T-C, Mendell J T, Salzberg S L, et al. StringTie enables improved reconstruction of a transcriptome from RNA-seq reads. Nature Biotechnology, 2015; 33(3): 290–295.

[45] Love M I, Huber W, Anders S. Moderated estimation of fold change and dispersion for RNA-seq data with DESeq2. Genome Biol, 2014; 15(12): 550.

[46] Gene Ontology Consortium. Gene Ontology: Tool for the unification of biology. Nat Genet, 2000; 25(1): 25–29.

[47] Kanehisa M, Goto S. KEGG: Kyoto Encyclopedia of Genes and Genomes. Nucleic Acids Res, 2000; 28(1): 27–30.

[48] Shen S, Park J W, Lu Z, Lin L, Henry M D, Wu Y N, et al. rMATS: Robust and flexible detection of differential alternative splicing from replicate RNA-Seq data. Proc Natl Acad Sci USA, 2014; 111(51): E5593–E5601.

[49] Gao J, Yu X, Ma F, Li J. RNA-Seq analysis of transcriptome and glucosinolate metabolism in seeds and sprouts of broccoli (*Brassica oleracea* var. Italica). PLoS ONE, 2014; 9(2): e88804.

[50] Lv Q, Liao J, Luo P, Zheng W, Liu J, Guo L, et al. Validation of suitable reference genes for qRT-PCR in cabbage (*Brassica oleracea* L.) under different abiotic stress experimental conditions. Plant Cell Rep, 2020; 39(5): 685–697.

[51] Livak K J, Schmittgen T D. Analysis of relative gene expression data using real-time quantitative PCR and the $2^{(-\Delta\Delta C_T)}$ method. Methods, 2001; 25(4): 402–408.

[52] Hassanien R H E, Ibrahim M M, Ghaly A E, Abdelrahman E N. Effect of photovoltaics shading on the growth of chili pepper in controlled greenhouses. Heliyon, 2022; 8(2): e08877.

[53] Liu Z, Peng T, Ma S, Qi C, Song Y, Zhang C, et al. Potential benefits and risks of solar photovoltaic power plants on arid and semi-arid ecosystems: an assessment of soil microbial and plant communities. Front Microbiol, 2023; 14: 1190650.

[54] Brouwer B, Gardeström P, Keech O. In response to partial plant shading, the lack of phytochrome A does not directly induce leaf senescence but alters the fine-tuning of chlorophyll biosynthesis. J Exp Bot, 2014; 65(14): 4037–4049.

[55] Petrakis T, Ioannou P, Kitsiou F, Kavga A, Grammatikopoulos G, Karamanos N. Growth and physiological characteristics of strawberry plants cultivated under greenhouse-integrated semi-transparent photovoltaics. Plants, 2024; 13(6): 768.

[56] Yang D L, Yao J, Mei C S, Tong X H, Zeng L J, Li Q, et al. Plant hormone jasmonate prioritizes defense over growth by interfering with gibberellin signaling cascade. Proc Natl Acad Sci USA, 2012; 109(19): E1192–E1200.

[57] Hu Y, Zhang X, Ma X. The influencing pathway of agrivoltaics on soybean protein concentration. Front Plant Sci, 2025; 16: 1618027.